Nonlinear Dyn (2017) 87:67–73
DOI 10.1007/s11071-016-3025-5

ORIGINAL PAPER

Rogue wave and combined breather with repeatedly excited behaviors in the dispersion/diffraction decreasing medium

Yue-Yue Wang · Chao-Qing Dai · Guo-Quan Zhou · Yan Fan · Liang Chen

Received: 25 May 2016 / Accepted: 14 August 2016 / Published online: 24 August 2016

Abstract A (3+1)-dimensional coupled nonlinear Schrödinger equation with different inhomogeneous diffractions and dispersion is investigated, and rogue wave and combined breather solutions are constructed. Different diffractions and dispersion of medium lead to the repeatedly excited behaviors of rogue wave and combined breather in the dispersion/diffraction decreasing system. These repeated behaviors including complete excitation, rear excitation, peak excitation and initial excitation are discussed.

Keywords Repeatedly excited behaviors · Rogue wave · Combined breather · (3+1)-dimensional coupled nonlinear Schrödinger equation

1 Introduction

In the last decades, considerable advances have been made in the investigation of solitons in various fields of physics and engineering [1–7]. In recent years, rogue waves (or freak waves)—single waves with amplitudes significantly larger than the surrounding waves—have also witnessed tremendous growth in various contexts of physics and engineering [8,9].

More recently, controllable behaviors of rogue waves and the related breathers have been studied [10–18]. The control for rogue waves [14] and superposed breather [15] were discussed. Controllable breather and Kuznetsov-Ma (KM) soliton trains in parity-time ($\mathcal{PT}$)-symmetric coupled waveguides have been reported [16]. Nonlinear tunneling effect of controllable combined KM soliton in $\mathcal{PT}$-symmetric nonlinear couplers has been discussed [17]. Controllable combined Peregrine soliton (PS) and KM soliton in $\mathcal{PT}$-symmetric nonlinear couplers have also been investigated [18].

In the periodic amplification system, the recurrence of PS with two peaks in a birefringent fiber with higher-order effects was reported [19]. Moreover, the recurrence of the combined PS and AB [20] and the recurrence of a KM soliton crossing Akhmediev breather (AB) [21] have also been studied in the periodic amplification system. These recurred behaviors in Refs. [19–21] originate from the periodic functions in the periodic amplification system.

In the diffraction/dispersion decreasing system (DDS), controllable behaviors of rogue waves [14,22] and breathers [21,23] were not reported to show the recurrence of excitation. However, we find that rogue wave and combined breather also possess the repeatedly excited behaviors in the DDS, which originates from different diffractions and dispersion of medium. The possibility of generation of the so-called nonlinear paired (or symbiotic) bright and dark solitons arising in the framework of the system of two coupled nonlinear Schrödinger equation (CNLSE) [24–26] was predicted. In this present paper, we study a (3+1)-dimensional

Y.-Y. Wang (✉) · C.-Q. Dai · G.-Q. Zhou · Y. Fan · L. Chen
School of Sciences, Zhejiang A&F University, Lin'an 311300, Zhejiang, People's Republic of China
e-mail: wangyy424@163.com

CNLSE with different inhomogeneous diffractions and dispersion and discuss repeated behaviors of symbiotic rogue wave and combined breather, including complete excitation, rear excitation, peak excitation and initial excitation.

2 Symbiotic rogue wave and breather solutions

In a real situation, the variation of the fiber geometry brings the inhomogeneity of medium [27]. When two optical fields u and v propagating in the same fiber are considered, the interactions between them are governed by the variable-coefficient CNLSE as follows:

$$
\begin{aligned}
&\mathrm{i}u_z + \frac{1}{2}\left[\beta_1(z)u_{xx} + \beta_2(z)u_{yy} + \beta_3(z)u_{tt}\right] \\
&\quad + \chi(z)(\sigma_{11}|u|^2 + \sigma_{12}|v|^2)u = \mathrm{i}\gamma(z)u, \\
&\mathrm{i}v_z + \frac{1}{2}\left[\beta_1(z)v_{xx} + \beta_2(z)v_{yy} + \beta_3(z)v_{tt}\right] \\
&\quad + \chi(z)(\sigma_{21}|u|^2 + \sigma_{22}|v|^2)v = \mathrm{i}\gamma(z)v,
\end{aligned} \tag{1}
$$

with two normalized complex mode fields $u(z, x, y, t)$ and $v(z, x, y, t)$, dimensionless propagation distance z and dimensionless transverse coordinates x, y and time t. The second and third terms in the left-hand sides denote the diffractions with different transverse coordinates (x, y), the fourth term represents dispersion, and the last two terms in the left-hand sides stand for the self-focusing ($\chi > 0$) or the self-defocusing ($\chi < 0$) nonlinearity with the self-phase-modulation (SPM) and cross-phase modulation (XPM). The constants $\sigma_{11}, \sigma_{12}, \sigma_{21}$ and σ_{22} determine the ratio of the coupling strengths of the XPM to the SPM. For linearly polarized eigenmodes $\sigma_{11} = \sigma_{22} = 1, \sigma_{12} = \sigma_{21} = 2/3$, whereas for circularly polarized modes $\sigma_{11} = \sigma_{22} = 1, \sigma_{12} = \sigma_{21} = 2$ with elliptically polarized eigenmodes $\sigma_{11} = \sigma_{22} = 1, 2 < \sigma_{12} = \sigma_{21} < 2/3$ [28]. These terms in the right-hand sides of Eq. (1) stand for the gain ($\gamma > 0$) or the loss ($\gamma < 0$).

Considering the relation between system parameters

$$
\begin{aligned}
\chi(z) = \frac{G}{4BA_0^2}&\left[\frac{k^2\beta_1(z)\alpha_2(z)\alpha_3(z)}{\alpha_1(z)}\right. \\
&\left. + \frac{l^2\beta_2(z)\alpha_1(z)\alpha_3(z)}{\alpha_2(z)} + \frac{m^2\beta_3(z)\alpha_1(z)\alpha_2(z)}{\alpha_3(z)}\right] \\
&\times \exp\left[-2\Gamma(z)\right],
\end{aligned} \tag{2}
$$

and using the following transformation

$$
\begin{aligned}
\begin{Bmatrix} u(z, x, y, t) \\ v(z, x, y, t) \end{Bmatrix} &= \begin{Bmatrix} \sqrt{\left|\frac{\sigma_{22}-\sigma_{12}}{\sigma_{12}\sigma_{21}-\sigma_{11}\sigma_{22}}\right|} \\ \sqrt{\left|\frac{\sigma_{11}-\sigma_{21}}{\sigma_{12}\sigma_{21}-\sigma_{11}\sigma_{22}}\right|} \end{Bmatrix} \\
&\times A(z)U[Z(z), X(z, x, y, t)] \exp[\mathrm{i}\phi(z, x, y, t)],
\end{aligned} \tag{3}
$$

with the amplitude $A(z) = A_0[\alpha_1(z)\alpha_2(z)\alpha_3(z)]^{1/2} \exp[\Gamma(z)]$, the effective propagation distance $Z(z) = \frac{1}{4B}[k^2\delta_1(z)\alpha_1(z) + l^2\delta_2(z)\alpha_2(z) + m^2\delta_3(z)\alpha_3(z)]$, the transformation variable $X(z, x, y, t) = \frac{1}{2}[k\alpha_1(z)x + l\alpha_2(z)y + m\alpha_3(z)t] - \frac{1}{2}[kd\delta_1(z)\alpha_1(z) + le\delta_2(z)\alpha_2(z) + mf\delta_3(z)\alpha_3(z)]$, the phase $\phi(z, x, y, t) = -\frac{1}{2}[a\alpha_1(z)x^2 + b\alpha_2(z)y^2 + c\alpha_3(z)t^2] + d\alpha_1(z)x + e\alpha_2(z)y + f\alpha_3(z)t - \frac{1}{2}[d^2\delta_1(z)\alpha_1(z) + e^2\delta_2(z)\alpha_2(z) + f^2\delta_3(z)\alpha_3(z)]$, the chirp factors $\alpha_1(z) = 1/[1 - a\delta_1(z)]$, $\alpha_2(z) = 1/[1 - b\delta_2(z)]$ and $\alpha_3(z) = 1/[1 - c\delta_3(z)]$, the accumulated diffractions $\delta_1(z) = \int_0^z \beta_1(s)\mathrm{d}s$, $\delta_2(z) = \int_0^z \beta_2(s)\mathrm{d}s$ and the accumulated dispersion $\delta_3(z) = \int_0^z \beta_3(s)\mathrm{d}s$, the accumulated gain/loss $\Gamma(z) = \int_0^z \gamma(s)\mathrm{d}s$ and constants $a, b, c, d, e, f, k, l, m$, Eq. (1) can be transformed into the famous NLSE with constant coefficients

$$
\mathrm{i}U_Z + \frac{B}{2}U_{XX} + G|U|^2U = 0, \tag{4}
$$

with two constants B and G. Here we choose $B = 1$ and $G = 1$.

From the transformation (3) and the modified Darboux transformation technique in Ref. [8], symbiotic rogue wave solution of Eq. (1) reads

$$
\begin{aligned}
\begin{Bmatrix} u(z, x, y, t) \\ v(z, x, y, t) \end{Bmatrix} &= \begin{Bmatrix} \sqrt{\left|\frac{\sigma_{22}-\sigma_{12}}{\sigma_{12}\sigma_{21}-\sigma_{11}\sigma_{22}}\right|} \\ \sqrt{\left|\frac{\sigma_{11}-\sigma_{21}}{\sigma_{12}\sigma_{21}-\sigma_{11}\sigma_{22}}\right|} \end{Bmatrix} \\
&\times A(z)\left[(-1)^n + \frac{M_n + \mathrm{i}(Z - Z_0)N_n}{L_n}\right] \\
&\times \exp\left\{\mathrm{i}\left[\left(1 - \frac{v^2}{2}\right)(Z - Z_0) + v_0X + \phi\right]\right\},
\end{aligned} \tag{5}
$$

where $2M_1 = L_1 = 8$, $N_1 = 1 + 4[X - v_0(Z - Z_0)]^2 + 4(Z - Z_0)^2$ for first-order rogue wave solution with $n = 1$ and $M_2 = [(X - v_0(Z - Z_0))^2 + (Z - Z_0)^2 + \frac{3}{4}][(X - v_0(Z - Z_0))^2 + 5(Z - Z_0)^2 + \frac{3}{4}] - \frac{3}{4}$, $N_2 = (Z - Z_0)\{(Z - Z_0)^2 - 3[X - v_0(Z - Z_0)]^2 + 2[(X - v_0(Z - Z_0))^2 + (Z - Z_0)^2]^2 - \frac{15}{8}\}$, $L_2 = \frac{1}{3}[(X - v_0$

$(Z-Z_0))^2+(Z-Z_0)^2]^3+\frac{1}{4}[(X-v_0(Z-Z_0))^2-3(Z-Z_0)^2]^2+\frac{9}{16}(X-v_0(Z-Z_0))^2+\frac{33}{16}(Z-Z_0)^2+\frac{3}{64}$ for second-order rogue wave with $n=2$, X, Z and ϕ are given below Eq. (3), and Z_0 and v_0 are two arbitrary constants.

Moreover, from the transformation (3) and the modified Darboux transformation technique in Ref. [9], symbiotic combined rogue wave and breather solution of Eq. (1) reads

$$\begin{Bmatrix} u(z,x,y,t) \\ v(z,x,y,t) \end{Bmatrix} = \begin{Bmatrix} \sqrt{\left|\frac{\sigma_{22}-\sigma_{12}}{\sigma_{12}\sigma_{21}-\sigma_{11}\sigma_{22}}\right|} \\ \sqrt{\left|\frac{\sigma_{11}-\sigma_{21}}{\sigma_{12}\sigma_{21}-\sigma_{11}\sigma_{22}}\right|} \end{Bmatrix} A(z)\left[1+\frac{G+\mathrm{i}F}{H}\right] \times \exp\left\{\mathrm{i}[(1-\frac{v^2}{2})(Z-Z_0)+v_0X+\phi]\right\}, \quad (6)$$

where $G=\kappa\{\kappa[\kappa^2(4Z_{s2}^2+4X_{s2}'^2+1)-8]\cosh(\delta Z_{s1})+8\delta\cos(\kappa X_{s1}')\}/8$, $F=\kappa\{8Z_{s2}[\delta\cos(\kappa X_{s1}')-\kappa\cosh(\delta Z_{s1})]+\delta\kappa(4Z_{s2}^2+4X_{s2}'^2+1)\sinh(\delta Z_{s1})\}/4$, $H=-\{\delta[\kappa^2(4Z_{s2}^2+4X_{s2}'^2+1)-16]\cos(\kappa X_{s1}')+\kappa([\kappa^2(4Z_{s2}^2+4X_{s2}'^2-3)+16]\cosh(\delta Z_{s1})-16\delta[Z_{s2}\sinh(\delta Z_{s1})+X_{s2}'\sin(\kappa X_{s1}')])\}/(4\kappa)$ with $Z_{s1}=Z-Z_0'$, $Z_{s2}=Z-Z_0$, $X_{s1}'=X_{s1}-v_0Z$, $X_{s2}'=X_{s2}-v_0Z$, $X_{sj}=X-X_j$, $\delta=\kappa\sqrt{4-\kappa^2}/2$, $\kappa=2\sqrt{1+n^2}$, $j=1,2$, with X, Z and ϕ being given below Eq. (3), an arbitrary constant v_0 and the modulation frequency κ. Z_0, Z_0' and X_j decide the center of solution in $Z-X$ coordinates. If $0<\mathrm{Im}(n)<1$ or $\mathrm{Im}(n)>1$ in solution (6), a rogue wave is combined by a breather or KM soliton, respectively. Here we choose $Z_0=Z_0'$ and $0<\mathrm{Im}(n)<1$; thus, solution (6) describes a rogue wave embedded on a breather.

As said in Refs. [29,30], nonautonomous solitons exist only under certain conditions and the parameter functions describing dispersion, nonlinearity and gain or absorption inhomogeneities cannot be chosen independently. Solutions (5) and (6) also exist under the relation between system parameters (2).

3 Repeatedly excited behaviors of rogue wave and combined breather

We consider repeatedly excited behaviors of rogue wave and combined breather in the following system with diffraction functions $\beta_1(z)$, $\beta_2(z)$ and dispersion function $\beta_3(z)$ as [31–33]

$$\beta_j(z)=\beta_{j0}\exp(-gz), \quad (7)$$

where positive parameters $\beta_{j0}(j=1,2,3)$ and g are related to diffraction or dispersion. When $g>0$, this system describes the exponential DDS.

As we all know, second-order rogue wave (5) reaches its peak at location $X=0$, $Z=Z_0$ and then gradually disappears in the $Z-X$ coordinates. Based on the expression of Z below Eq. (3) and (7), we obtain $Z=k^2\beta_{10}[1-\exp(-gz)]/[4g-4a\beta_{10}(1-\exp(-gz))]+l^2\beta_{20}[1-\exp(-gz)]/[4g-4b\beta_{20}(1-\exp(-gz))]+m^2\beta_{30}[1-\exp(-gz)]/[4g-4c\beta_{30}(1-\exp(-gz))]$, which hints that the value of Z approaches the maximum value $Z_m=k^2\beta_{10}/[4(g-a\beta_{10})]+l^2\beta_{20}/[4(g-b\beta_{20})]+m^2\beta_{30}/[4(g-c\beta_{30})]$ as z approaches infinity. The degree of excitation of second-order rogue wave is decided by the relation between the maximum Z_m and peak location Z_0.

When $Z_m=Z_0$, the critical value of g can be obtained if other parameters are chosen as certain values. If parameters are chosen as $k=0.9$, $l=1$, $m=1.1$, $a=0.45$, $b=0.5$, $c=0.55$, $\beta_{10}=0.25$, $\beta_{20}=0.3$, $\beta_{30}=0.35$, $Z_m=Z_0=6$ produces triple roots of parameter g, namely $g_1=0.1177$, $g_2=0.1593$, $g_3=0.2166$. We find that Z_m non-montonically changes, that is, Z_m increases and decreases again and again. Therefore, repeatedly excited behaviors of rogue wave will happen in the DDS.

In the following, we discuss repeatedly excited behaviors for one of component u from the symbiotic solution. Actually, similar repeatedly excited behaviors will also happen for another component v of the symbiotic solution.

Figure 1 displays repeatedly excited behaviors of rogue wave with the add of values of g in the DDS. If $g=0.115<g_1$ in Fig. 1a, then $Z_m>Z_0$; thus, the complete second-order rogue wave is excited. If $g=0.1177=g_1$ in Fig. 1b, then $Z_m=Z_0$; thus, the second-order rogue wave is excited to the peak and self-similarly sustains its peak along the propagation distance. If $g=0.14>g_1$, then $Z_m<Z_0$ in Fig. 1c; thus, the threshold of exciting a complete rogue wave is never reached, and the rogue wave is only excited to the initial part. If $g_1<g=0.15<g_2$ in Fig. 1d, then $Z_m>Z_0$ again; thus, the full second-order rogue wave is excited again. If $g_1<g=0.1593=g_2$ in Fig. 1e, the maintenance of peak excitation of rogue wave happens once again. If $g=0.17>g_2$ in Fig. 1f, the complete excitation

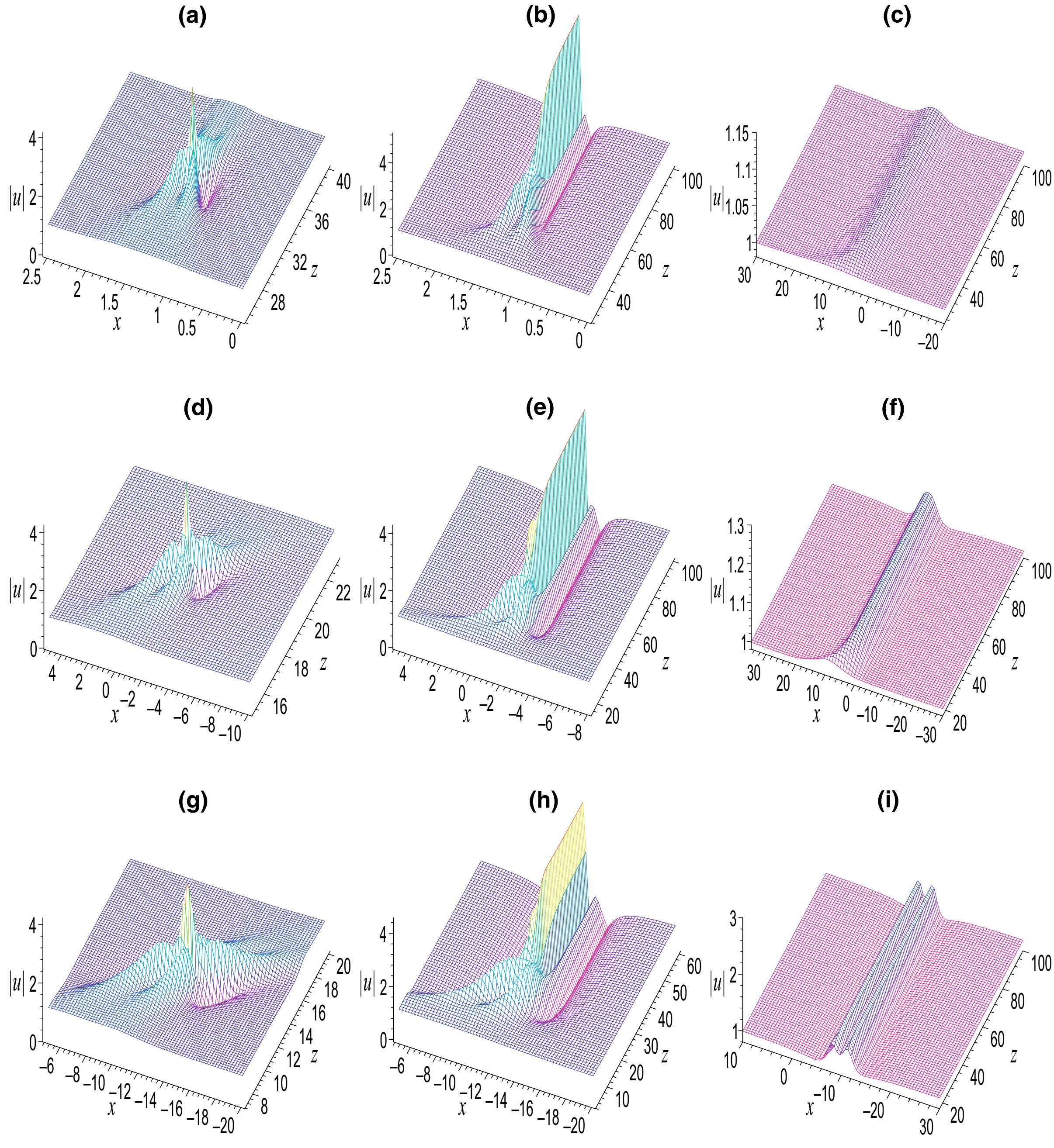

Fig. 1 **a**, **d**, **g** complete excitation, **b**, **e**, **h** peak excitation, and **c**, **f**, **i** initial excitation of the second-order rogue wave in the DDS, respectively. Parameters are chosen as $A_0 = 0.5, k = 0.9, l = 1, m = 1.1, a = d = 0.45, b = e = 0.5, c = f = 0.55, \beta_{10} = 0.25, \beta_{20} = 0.3, \beta_{30} = 0.35, Z_0 = 6, v_0 = 0.1, \sigma_{12} = \sigma_{21} = 1.5, \sigma_{11} = \sigma_{22} = 1$ with **a** $g = 0.115$, **b** $g = 0.1177$, **c** $g = 0.14$, **d** $g = 0.15$, **e** $g = 0.1593$, **f** $g = 0.17$, **g** $g = 0.2$, **h** $g = 0.2166$ and **i** $g = 0.23$, respectively. We take $y = 2, t = 3$. Results are similar for other values of y and t

is restrained, and rogue wave is initially excited. If $g_2 < g = 0.2 < g_3$ in Fig. 1g, $g = 0.2166 = g_3$ in Fig. 1h and $g = 0.23 > g_3$ in Fig. 1i, the complete excitation, peak excitation and initial excitation of the second-order rogue wave will appear again. This phenomenon of repeated excitation has not been reported

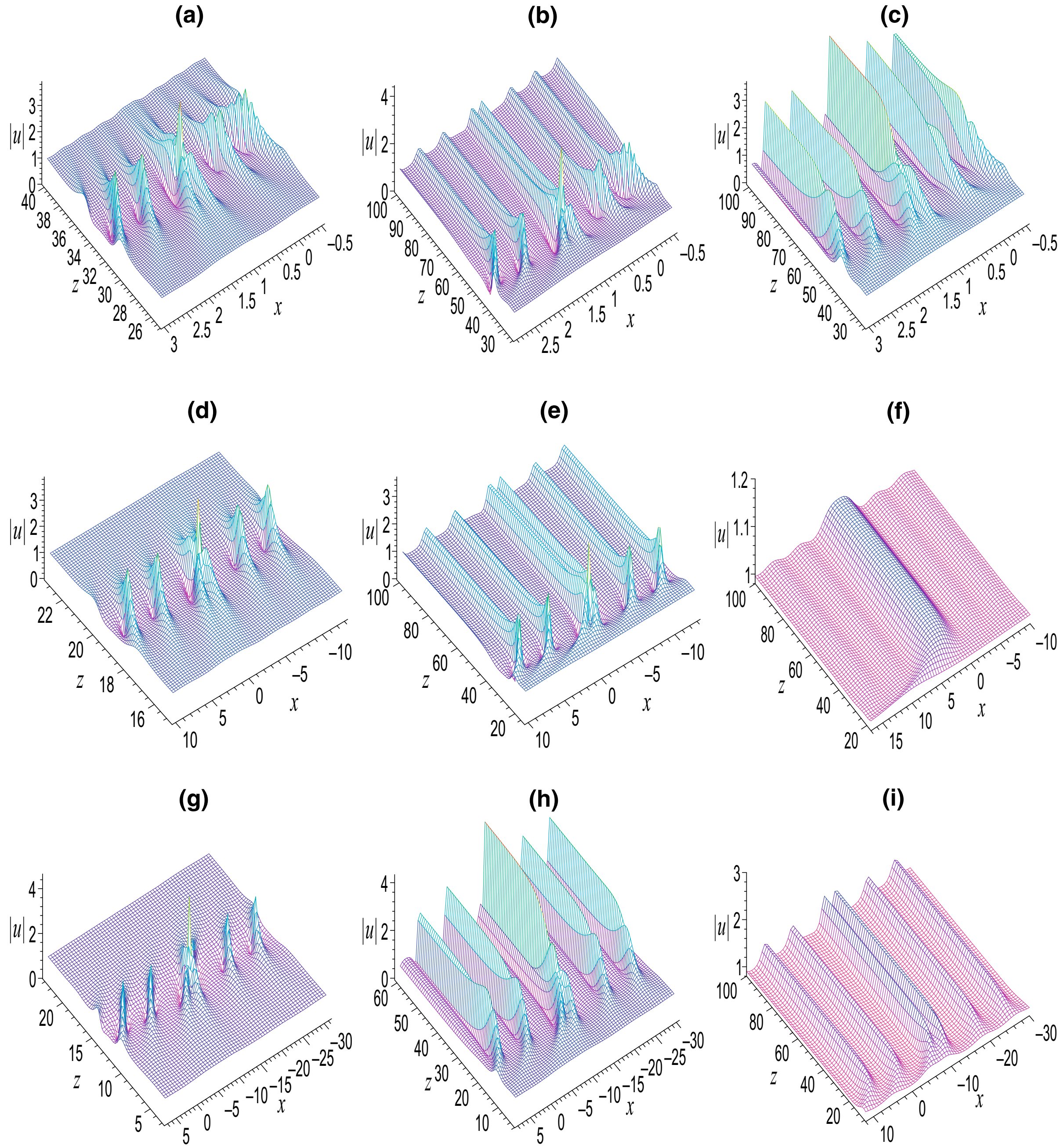

Fig. 2 **a**, **d**, **g** complete excitation, **b**, **e** rear excitation, **c**, **h** peak excitation and **f**, **i** initial excitation of a rogue wave embedded on a breather in the DDS, respectively. Parameters are chosen as the same as those in Fig. 1 except for $n = 0.85\mathrm{i}$, $X_1 = X_2 = 0$ with **a** $g = 0.115$, **b** $g = 0.117$, **c** $g = 0.1177$, **d** $g = 0.15$, **e** $g = 0.158$, **f** $g = 0.17$, **g** $g = 0.2$, **h** $g = 0.2166$ and **i** $g = 0.23$, respectively. We take $y = 2$, $t = 3$. Results are similar for other values of y and t

in the system with same diffractions and dispersion in Ref. [34].

Similar case of repeated excitation also happens for a rogue wave embedded on a breather. In the $Z - X$ coordinates, the rogue wave and breather in solution (6) altogether reach their peaks at location $X = 0$, $Z = Z_0$ and then gradually disappear. Adjusting the relation between Z_m and Z_0, we can also discuss controllable excitation of the rogue wave embedded on a breather.

Figure 2 exhibits repeatedly excited behaviors of the rogue wave embedded on a breather with the add of values of g in the DDS. If $g = 0.115 < g_1$ in Fig. 2a, then $Z_m > Z_0$; thus, the complete excitation of the rogue wave embedded on a breather appears. If $g = 0.117$ (a bit smaller than g_1) in Fig. 2b, rogue wave and breather are all excited rear part, and the rear part of rogue wave and breather do not disappear along z. If $g = 0.1177 = g_1$ in Fig. 2c, then $Z_m = Z_0$; thus, the rogue wave and breather are all excited to their peaks and self-similarly maintain their maximum amplitudes along the propagation distance. If $g > g_1$, the complete excitation of the rogue wave embedded on a breather is restrained. If $g_1 < g = 0.15 < g_2$ in Fig. 2d, then $Z_m > Z_0$ again; thus, the rogue wave embedded on a breather is excited again. If $g = 0.158$ (a bit smaller than g_2) in Fig. 2e, the rear excitation of rogue wave and breather happens again, and the rogue wave embedded on a breather propagates along z with a tail. If $g = g_2$, the maintenance of peak excitation of rogue wave happens once again. If $g = 0.17 > g_2$ in Fig. 2f, the complete excitation is restrained, and the rogue wave embedded on a breather is initially excited. If $g_2 < g = 0.2 < g_3$ in Fig. 2g, $g = 0.2166 = g_3$ in Fig. 2h and $g = 0.23 > g_3$ in Fig. 2i, the complete excitation, peak excitation and initial excitation of the rogue wave embedded on a breather will also happen. This phenomenon of repeated excitation has not been reported in the system with same diffractions and dispersion in Ref. [35]. Therefore, different diffractions and dispersion of medium lead to the repeatedly excited behaviors of rogue wave and combined breather in the DDS.

4 Summary

In summary, we investigate a (3+1)-dimensional CNLSE with different inhomogeneous diffractions and dispersion and construct rogue wave and combined breather solutions. From the relation between the transformation variable Z and real distance z, we obtain the maximum value of Z_m in DDS. Comparing values of Z_m and peak location Z_0, we study complete excitation, rear excitation, peak excitation and initial excitation of rogue wave and combined breather. In DDS, a new phenomenon of repeatedly excited behaviors is discussed. The reason to appear these repeatedly excited behaviors is the existence of different diffractions and dispersion of medium. These repeated behaviors including complete excitation, rear excitation, peak excitation and initial excitation are discussed.

Acknowledgements This work was supported by the Zhejiang Provincial Natural Science Foundation of China (Grant Nos. Y17A040042, Y17F050046 and LY16A040014) and the National Natural Science Foundation of China (Grant Nos. 11375007, 11404289 and 11574272). Dr. Chao-Qing Dai is also sponsored by the Foundation of New Century "151 Talent Engineering" of Zhejiang Province of China and Youth Top-notch Talent Development and Training Program of Zhejiang A&F University.

References

1. Zhou, Q., Yu, H., Xiong, X.: Optical solitons in media with time-modulated nonlinearities and spatiotemporal dispersion. Nonlinear Dyn. **80**, 983–987 (2015)
2. Guo, R., Liu, Y.F., Hao, H.Q., Qi, F.H.: Coherently coupled solitons, breathers and rogue waves for polarized optical waves in an isotropic medium. Nonlinear Dyn. **80**, 1221–1230 (2015)
3. Chen, Y.X., Xu, F.Q., Jiang, B.Y.: Spatiotemporal soliton structures in (3+ 1)-dimensional PT-symmetric nonlinear couplers with gain and loss. Nonlinear Dyn. **82**, 2051–2057 (2015)
4. Mani Rajan, M.S., Mahalingam, A.: Nonautonomous solitons in modified inhomogeneous Hirota equation. Nonlinear Dyn. **79**, 2469–2484 (2015)
5. Zhu, H.P., Pan, Z.H.: Vortex soliton in (2+1)-dimensional PT-symmetric nonlinear couplers with gain and loss. Nonlinear Dyn. **83**, 1325–1330 (2016)
6. Xu, Y.J.: Hollow ring-like soliton and dipole soliton in (2+ 1)-dimensional PT-symmetric nonlinear couplers with gain and loss. Nonlinear Dyn. **83**, 1497–1501 (2016)
7. Wu, H.Y., Jiang, L.H.: Vector Hermite–Gaussian spatial solitons in (2+1)-dimensional strongly nonlocal nonlinear media. Nonlinear Dyn. **83**, 713–718 (2016)
8. Akhmediev, N., Ankiewicz, A., Taki, M.: Waves that appear from nowhere and disappear without a trace. Phys. Lett. A **373**, 675–678 (2009)
9. Kedziora, D.J., Ankiewicz, A., Akhmediev, N.: Second-order nonlinear Schrodinger equation breather solutions in the degenerate and rogue wave limits. Phys. Rev. E **85**, 066601 (2012)
10. Yang, Z.P., Zhong, W.P., Belic, M.: 2D optical rogue waves in self-focusing Kerr-type media with spatially modulated coefficients. Laser Phys. **25**, 085402 (2015)
11. Zhong, W.P., Belic, M., Huang, T.W.: Rogue wave solutions to the generalized nonlinear Schrödinger equation with variable coefficients. Phys. Rev. E **87**, 065201 (2013)
12. Zhong, W.P.: Rogue wave solutions of the generalized one-dimensional Gross–Pitaevskii equation. J. Nonlinear Opt. Phys. Mater. **21**, 1250026 (2012)

13. Zhong, W.P., Belic, M., Zhang, Y.Q.: Second-order rogue wave breathers in the nonlinear Schrödinger equation with quadratic potential modulated by a spatially-varying diffraction coefficient. Opt. Express **23**, 3708–3716 (2015)
14. Dai, C.Q., Wang, Y.Y., Tian, Q., Zhang, J.F.: The management and containment of self-similar rogue waves in the inhomogeneous nonlinear Schrodinger equation. Ann. Phys. **327**, 512–521 (2012)
15. Dai, C.Q., Wang, Y.Y.: Superposed Akhmediev breather of the (3+1)-dimensional generalized nonlinear Schrödinger equation with external potentials. Ann. Phys. **341**, 142–152 (2014)
16. Dai, C.Q., Wang, Y.Y., Zhang, X.F.: Controllable Akhmediev breather and Kuznetsov-Ma soliton trains in PT-symmetric coupled waveguides. Opt. Express **22**, 29862–29867 (2014)
17. Chen, Y.X., Jiang, Y.F., Xu, Z.X., Xu, F.Q.: Nonlinear tunnelling effect of combined Kuznetsov-Ma soliton in (3+1)-dimensional PT-symmetric inhomogeneous nonlinear couplers with gain and loss. Nonlinear Dyn. **82**, 589–597 (2015)
18. Dai, C.Q., Wang, Y.Y.: Controllable combined Peregrine soliton and Kuznetsov–Ma soliton in PT-symmetric nonlinear couplers with gain and loss. Nonlinear Dyn. **80**, 715–721 (2015)
19. Li, J.T., Han, J.Z., Du, Y.D., Dai, C.Q.: Controllable behaviors of Peregrine soliton with two peaks in a birefringent fiber with higher-order effects. Nonlinear Dyn. **82**, 1393–1398 (2015)
20. Li, J.T., Zhang, X.T., Meng, M., Liu, Q.T., Wang, Y.Y., Dai, C.Q.: Control and management o f the combined Peregrine soliton and Akhmediev breathers in PT-symmetric coupled waveguides. Nonlinear Dyn. **84**, 473–479 (2016)
21. Chen, H.Y., Zhu, H.P.: Controllable behaviors of spatiotemporal breathers in a generalized variable-coefficient nonlinear Schrodinger model from arterial mechanics and optical fibers. Nonlinear Dyn. **81**, 141–149 (2015)
22. Dai, C.Q., Zhou, G.Q., Zhang, J.F.: Controllable optical rogue waves in the femtosecond regime. Phys. Rev. E **85**, 016603 (2012)
23. Zhu, H.P.: Spatiotemporal breather in diffraction decreasing media. Wave Motion **51**, 438–444 (2014)
24. Afanasyev, V.V., Dianov, E.M., Prokhorov, A.M., Serkin, V.N.: Nonlinear pairing of light and dark optical solitons. JETP Lett. **48**, 638–642 (1988)
25. Afanasyev, V.V., Kivshar, YuS, Konotop, V.V., Serkin, V.N.: Dynamics of coupled dark and bright optical solitons. Opt. Lett. **14**, 805–807 (1989)
26. Kivshar, YuS, Anderson, D., Hook, A., Lisak, M., Afanasjev, A.A., Serkin, V.N.: Symbiotic optical solitons and modulational instability. Phys. Scr. **44**, 195–202 (1991)
27. Abdullaeev, F.: Theory of Solitons in Inhomogeneous Media. Wiley, New York (1994)
28. Cao, X.D., Meyerhofer, D.D.: Soliton collisions in optical birefringent fibers. J. Opt. Soc. Am. B **11**, 380–385 (1994)
29. Serkin, V.N., Hasegawa, A.: Novel soliton solutions of the nonlinear Schrodinger equation model. Phys. Rev. Lett. **85**, 4502–4505 (2000)
30. Serkin, V.N., Hasegawa, A.: Soliton management in the nonlinear Schrödinger equation model with varying dispersion, nonlinearity, and gain. JETP Lett. **72**, 89–92 (2000)
31. Serkin, V.N., Hasegawa, A.: Exactly integrable nonlinear Schrodinger equation models with varying dispersion, nonlinearity and gain: application for soliton dispersion management. IEEE J. Sel. Top. Quant. Electron. **8**, 418–431 (2002)
32. Serkin, V.N., Belyaeva, T.L.: High-energy optical Schrödinger solitons. JETP Lett. **74**, 573 (2001)
33. Dai, C.Q., Wang, Y.Y.: Spatiotemporal localizations in (3+1)-dimensional PT-symmetric and strongly nonlocal nonlinear media. Nonlinear Dyn. **83**, 2453–2459 (2016)
34. Dai, C.Q., Wang, X.G., Zhang, J.F.: Nonautonomous spatiotemporal localized structures in the inhomogeneous optical fibers: interaction and control. Ann. Phys. **326**, 645–656 (2011)
35. Zhou, G.Q., Dai, C.Q., Chen, Y.X.: Nonlinear tunnelling of superposed Akhmediev breather in PT-symmetric inhomogeneous nonlinear couplers with gain and loss. Opt. Commun. **345**, 31–36 (2015)